Tuning the Fermi level beyond the equilibrium doping limit through quenching: The case of CdTe

Ji-Hui Yang,[1] Ji-Sang Park,[1] Joongoo Kang,[2] Wyatt Metzger,[1] Teresa Barnes,[1] and Su-Huai Wei[1,*]
[1]*National Renewable Energy Laboratory, Golden, Colorado 80401, USA*
[2]*Department of Emerging Materials Science, DGIST, Daegu 711-873, Korea*
(Received 2 September 2014; revised manuscript received 21 November 2014; published 8 December 2014)

The Fermi level of a material is a fundamental quantity that determines its electronic properties. Thus, the ability to tune Fermi levels is important for developing electronic device materials. However, for most materials, the Fermi level is limited to a certain range in the band gap due to the existence of certain intrinsic compensating defects. Here we demonstrate that quenching can be used as an effective way to overcome this limit, allowing the Fermi levels to be tuned in a much wider range. Taking a photovoltaic material CdTe as a prototype example, we analyzed the physical origin of Fermi level pinning and explained why growing the sample at high temperature followed by rapid quenching to room temperature can overcome the self-compensation limit. We further show that for CdTe, quenching can increase the Fermi level range from about 0.6 to 1.1 eV, which has a great potential in improving CdTe solar cell performance. Our proposed strategy of tuning Fermi level positions beyond the intrinsic equilibrium doping limit is general and can be applied to other semiconductor systems.

DOI: 10.1103/PhysRevB.90.245202 PACS number(s): 61.72.uj, 61.72.Bb, 61.72.J−, 71.55.Gs

I. INTRODUCTION

The Fermi level position (E_F) of a material is a fundamental quantity that plays a key role in determining its functionality. Therefore, it is desirable that E_F can be well controlled and tuned in a wide range to satisfy requirements for some specific applications. For example, in topological insulators, E_F needs to be controlled close to the Dirac point for physical studies and practical applications [1–4]. In thermoelectric materials, E_F should be tuned to maximize the figure of merits [5–8]. In photovoltaic (PV) materials, E_F needs to be tuned in a range as large as possible to obtain high diffuse voltages, which give high open circuit voltages. It is well known that for a pristine material with the exact stoichiometry, E_F is pinned near the middle of the band gap, because the amounts of thermally excited electrons and holes are always the same. In reality, intrinsic defects are formed during material growth and E_F can vary in a certain range by controlling the growth conditions. However, due to the self-compensation effect, the variation of E_F is often limited: Outside of a certain E_F range, some compensating defects can form more easily than others, thus returning E_F back under the equilibrium growth conditions. So far, most of the studies on overcoming the doping limit [9–18] focus on enhancing solubility of desirable intrinsic defects under equilibrium growth conditions or on obtaining proper transition energy levels through codoping or extrinsic doping. Little was discussed about overcoming Fermi level pinning. The importance of E_F in electronic applications necessitates the exploration of new approaches for overcoming the doping limit and tuning E_F more efficiently.

Specifically, in PV materials such as CdTe, $Cu(In,Ga)Se_2$, and $Cu_2ZnSn(S,Se)_4$, E_F is required to cover a range as large as possible, which means E_F^n and E_F^p, the Fermi energy levels referenced to the valence band maximum (VBM) for n-type and p-type doped layers, respectively, need to be tuned towards as close as possible to the respective band edges. Because the difference $\phi_D = (E_F^n - E_F^p)/q$, where q is electron charge and ϕ_D is the diffusion voltage at the homogeneous p-n junction of this material (Fig. 1), is proportionally related to the open circuit voltage (V_{OC}) of the solar cells. However, under equilibrium intrinsic growth conditions, the variation of E_F^p or E_F^n are often limited, especially if some defects have very low formation energies. For example, antisite cation acceptors in multication compounds [19,20] can form easily, which pins the E_F^n close to the VBM, leading to small ϕ_D and V_{OC} compared to their band gaps [21]. These deficiencies of V_{OC} have now become hindrances for the further improvement of these solar cells' performances.

Here we take CdTe as a prototype system to reveal the origins of Fermi level pinning and to discuss possible strategies for increasing the range of E_F beyond intrinsic limits. As one of the most important thin-film solar cell materials with relatively low cost and high efficiency, CdTe has recently reached an efficiency of 20.4% by First Solar [22]. However, this is still far from its theoretical maximum efficiency (∼30%). A major limiting factor is its low V_{OC}, which is only about 0.85 eV, much smaller than its band gap. Therefore, to further improve CdTe solar cell efficiency, reasons behind such a small V_{OC} need to be revealed and possible solutions are suggested.

In this paper we first investigate the intrinsic defect properties of CdTe using first-principles calculations and explain why V_{OC} of CdTe solar cell is small. Then using thermodynamical theory of defects, we quantitatively study the Fermi level splitting in CdTe under equilibrium growth conditions. By understanding the Fermi level splitting mechanism, we propose a nonequilibrium quenching method for overcoming the E_F and V_{OC} limitation. Our quantitative study shows that ϕ_D of CdTe solar cell can reach as high as 1.1 eV after quenching, which has great potential to improve the energy conversion efficiency.

II. CALCULATION METHODS

Our first-principles total energy and band structure calculations were performed using density functional theory (DFT) [23,24] as implemented in the VASP code [25,26]. The electron

*Suhuai.Wei@nrel.gov

 ©2014 American Physical Society

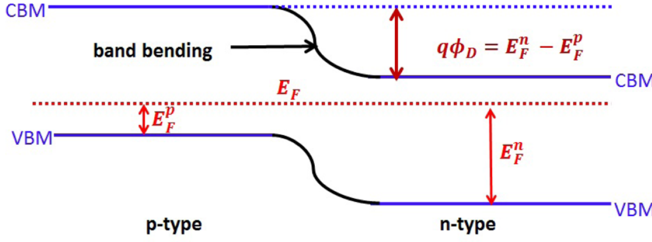

FIG. 1. (Color online) Schematic diagram to show that diffusion voltage ϕ_D is determined by the Fermi level differences $q\phi_D = E_F^n - E_F^p$, which is bounded by the band gap of the material.

and core interactions are included using the frozen-core projected augmented wave (PAW) approach [27]. To correct the band gap error, the Heyd-Scuseria-Ernzerhof (HSE06) hybrid functional [28] is used. The defect calculations are performed within a 64-atom supercell where all the atoms in the supercell are fully relaxed till the forces on every atom are less than 0.05 eV/Å. The total energy is calculated with $2 \times 2 \times 2$ Monkhorst-Pack special k-point meshes and Gaussian smearing method (SIGMA = 0.02) to make sure it is converged within 0.1 eV using an energy cutoff of 300 eV. The defect properties are calculated using the scheme in Ref. [9]. Using the HSE06 functional with the default exchange parameters ($\alpha = 0.25$), the calculated lattice constant of pure CdTe is 6.58 Å with a band gap of 1.49 eV, in good agreement with the experiments [29].

III. INTRINSIC DEFECT PROPERTIES OF CdTe

Figure 2 shows the intrinsic defect formation energies as a function of E_F under Cd-rich and Te-rich growth conditions. Compared to previous calculations [11], our results mainly show two different characters. First, the transition energy level of Cd vacancy from 0 to −2 is 0.36 eV above the valence band maximum (VBM) of CdTe, making it a relatively deep acceptor. The relatively deep acceptor level is caused by the large

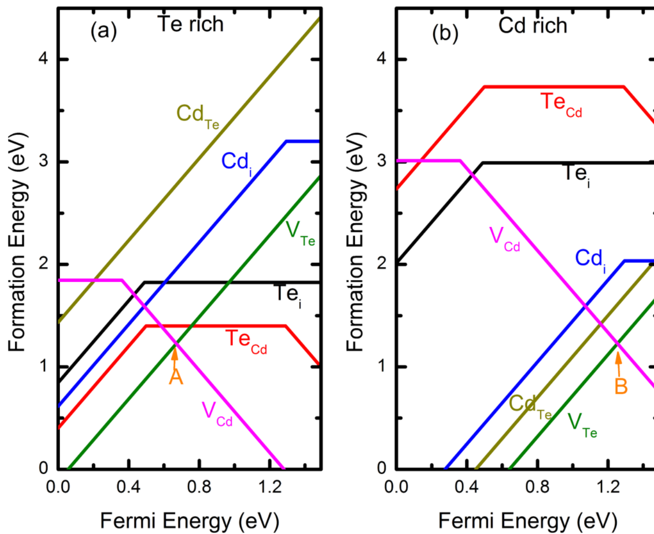

FIG. 2. (Color online) Intrinsic defect formation energies versus Fermi levels in CdTe under (a) Te rich conditions and (b) Cd-rich conditions.

local structure distortion around V_{Cd} at the neutral charge state, where two Te get closer and the other two Te get farther, thus splitting the threefold degenerated defect states under T_d symmetry to two degenerated fully occupied states and one unoccupied state. The upshift of this unoccupied state makes it cost more energy to accept two electrons from VBM, leading to the relatively deep transition level of V_{Cd}. Another different result is that V_{Te} becomes a rather shallow and dominant donor with the (2+/0) transition energy level above the conduction band minimum (CBM). This shallow donor level is caused by large atomic displacement of Cd atoms around this defect when the defect becomes charged [30]. We see that, under equilibrium growth conditions, E_F^p will be bounded around point A and E_F^n will be bounded around point B, yielding a diffuse voltage of about 0.6 eV. The exact Fermi energy at finite temperature, however, will depend on the generated defect densities as well as thermally excited electron and hole concentrations.

IV. THERMODYNAMIC SIMULATIONS UNDER EQUILIBRIUM GROWTH CONDITIONS

Under thermodynamic equilibrium growth conditions and within the dilute limit, the density of a defect α with charge state q can be calculated as

$$n(\alpha,q) = N_{\mathrm{site}} g_q e^{-\Delta H_f(\alpha,q)/k_B T}, \tag{1}$$

where N_{site} is the number of possible sites per volume for defect α, g_q is the degeneracy factor related to possible electron occupations [31,32], and $\Delta H_f(\alpha,q)$ is the formation energy of a defect α at charge state q. Here $\Delta H_f(\alpha,q)$ is defined as [9]

$$\Delta H_f(\alpha,q) = E(\alpha,q) - E(\mathrm{host}) + \sum_i n_i(E_i + \mu_i) + q[\varepsilon_{\mathrm{VBM}}(\mathrm{host}) + E_F], \tag{2}$$

which is a function of chemical potentials μ_i of involved elements and Fermi level E_F. At a given temperature, the thermally excited electron density n_0 and hole density p_0 are also functions of Fermi level, which are given as

$$\begin{aligned} n_0 &= N_c e^{-\frac{E_c - E_F}{k_B T}}, \quad N_c = 2\frac{(2\pi m_n^* k_B T)^{3/2}}{h^3}, \\ p_0 &= N_v e^{-\frac{E_F - E_v}{k_B T}}, \quad N_v = 2\frac{(2\pi m_p^* k_B T)^{3/2}}{h^3}. \end{aligned} \tag{3}$$

Here N_c is the temperature-dependent effective density of states of the conduction band that can accept electrons and N_v is the effective density of states of the valence band that can accept holes. m_n^* (0.095 m_0 for CdTe) and m_p^* (0.84 m_0 for CdTe) are effective masses of electrons and holes, taking into account of spin degeneracy and spin-orbital coupling [32,33]. The neutralization condition in a semiconductor system with defects requires that

$$p_0 + \sum_i q_i\, n_{D_i}^{q_i+} = n_0 + \sum_j q_j n_{A_j}^{q_j-}, \tag{4}$$

where $n_{D_i}^{q_i+}$ is the density of a donor D_i with charge state q_i and $n_{A_j}^{q_j-}$ is the density of an acceptor A_j with charge state $-q_j$. By solving equations in Eqs. (1)–(4) self-consistently, we can

obtain the E_F of a semiconductor system at given chemical potentials, as well as carrier densities and defect densities, when this material is grown under equilibrium conditions at a given growth temperature.

Our simulations for CdTe are shown in Fig. 3. As can be seen in the left panels, at $T = 300$ K, the Fermi level of CdTe is generally pinned in the middle of the band gap [Fig. 3(a)]. This is because equilibrium defect densities in CdTe are very low ($<10^6/\mathrm{cm}^3$) at this temperature so intrinsic thermal excitation process dominate with $N_c \sim 10^{17}/\mathrm{cm}^3$ and $N_v \sim 10^{19}/\mathrm{cm}^3$. As the growth temperature increases to 800 and 1200 K, more defects can be created and band edge excitation becomes less dominant, so the E_F is pushed down for p-type doping (under Cd-poor conditions) or up for n-type doping (under Cd-rich conditions), enlarging the variation range of E_F. Notice that the E_F only shifts slightly even though the defect density has increased by more than ten orders of magnitude. This is because the effective band edge density of states and band to band thermal excitation also increase significantly at a high temperature, so the E_F is still primarily controlled by the band edge excitation. However, no matter how high the growth temperature is, the E_F will be pinned around 0.7 eV or near position A in Fig. 2(a) for p-type doping, which is the lowest E_F achievable for p-type CdTe under thermodynamic equilibrium growth conditions. This is because if E_F is lower than A, the formation energy of V_{Te}^{2+} would be lower than that of V_{Cd}^{2-}, thus more V_{Te}^{2+} would form than V_{Cd}^{2-}, pushing the Fermi level up. Similarly, for n-type doping, the Fermi level will be pinned around 1.3 eV or position B in Fig. 2(b), which is the highest Fermi level for n-type CdTe under equilibrium growth conditions. As a result of this intrinsic self-doping limit, the largest possible ϕ_D of CdTe solar cells grown under equilibrium conditions will be limited by the Fermi level difference between the two pinning points A and B, which is only about 0.6 eV.

To overcome the Fermi energy limit and widen the E_F range, other methods such as nonequilibrium growth approaches should be considered. Notice that the shift of E_F is determined largely by the excess electrons or holes from the dominant intrinsic defects. To increase excess carriers from a particular intrinsic defect, high temperatures are often necessary to simultaneously generate the defects and shift the E_F to a desirable position. However, to increase electrons-to-holes ratio and shift the E_F towards the band edges, thermal excitations from the band edges must be reduced, which can only be achieved at a low temperature. Therefore, quenching may be a strategy to overcome the E_F pinning caused by defect self-compensation. After quenching at a given growth chemical potential, intrinsic defects can dominate over thermal excitations and one type of defect (acceptor or donor) can dominate over the others, thus shifting the E_F to either its acceptor transition energy level and valence band or its donor transition energy level and conduction band.

V. THERMODYNAMIC SIMULATIONS AFTER QUENCHING

When rapidly quenching to a low temperature (e.g., room temperature), the total density of a defect α generated at a high temperature, which is the sum of densities of α with all possible

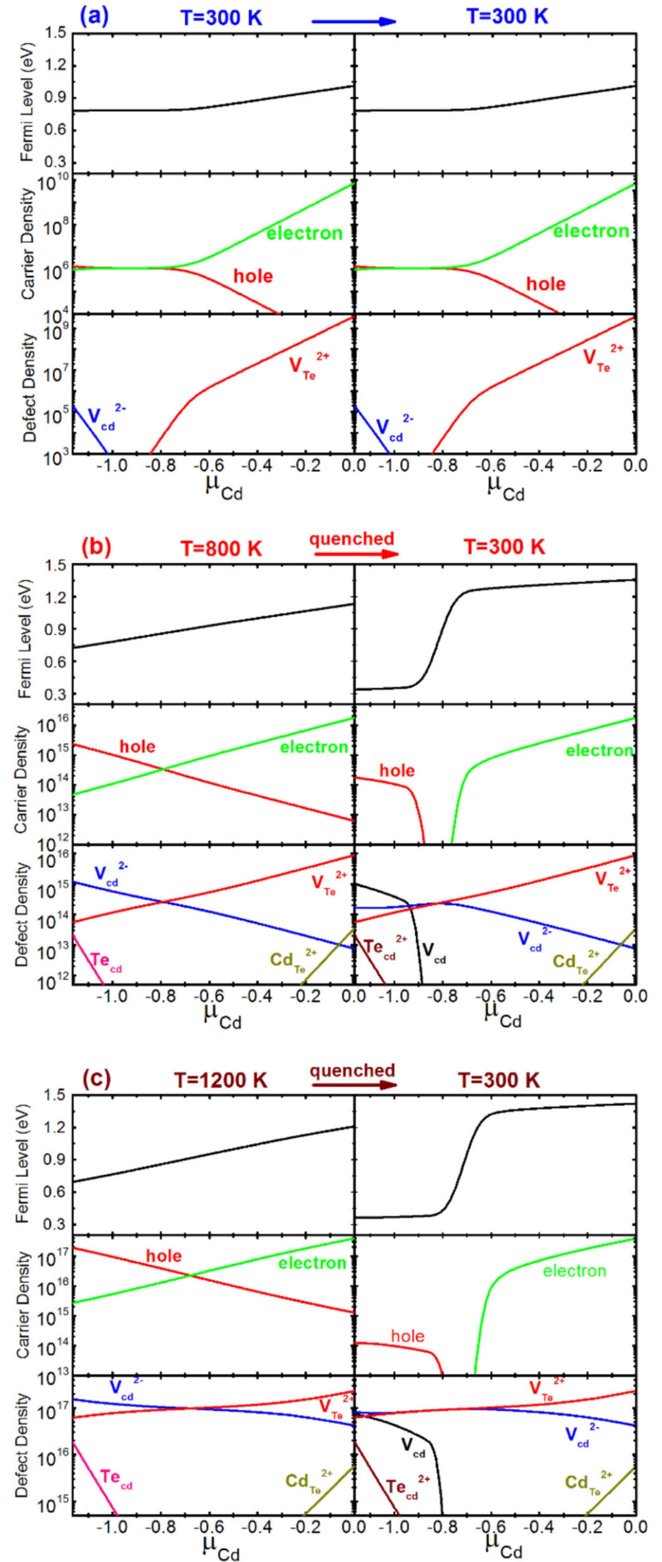

FIG. 3. (Color online) Fermi level, carrier density, and defect density as functions of Cd chemical potential under thermodynamic equilibrium growth condition are shown in the left panels of (a) at $T = 300$ K, (b) at $T = 800$ K, and (c) at $T = 1200$ K. The right panels of (a)–(c) show the quenched (to $T = 300$ K) Fermi level, carrier density, and defect density as functions of Cd chemical potential.

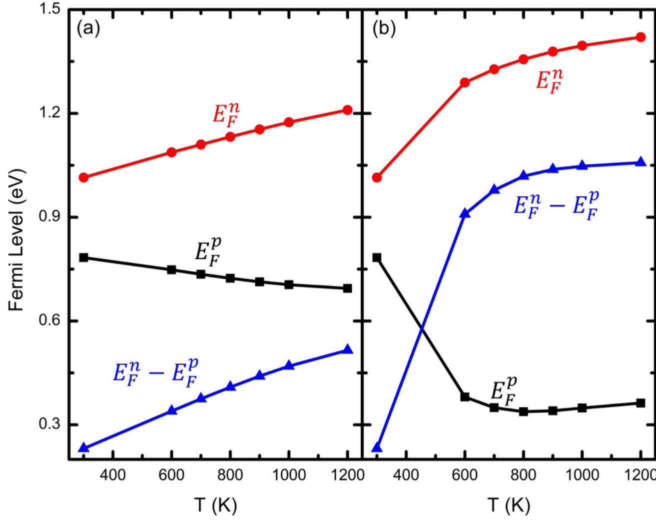

FIG. 4. (Color online) (a) Under thermodynamic equilibrium conditions, E_F^p (under Cd-poor condition), E_F^n (under Cd-rich condition), and their differences $E_F^n - E_F^p$ as a function of growth temperatures. (b) The same properties after quenching to room temperature.

charge states, is assumed to be unchanged. The only possible change after the rapid quenching is the redistribution of defect densities at different charge states. For example, considering a defect α with two charge states 0 and q, the density of α with charge state q is recalculated as

$$n'(\alpha,q) = N_\alpha \frac{g_q e^{-\Delta H_f(\alpha,q)/k_B T}}{g_q e^{-\Delta H_f(\alpha,q)/k_B T} + g_0 e^{-\Delta H_f(\alpha,0)/k_B T}}, \quad (5)$$

where N_α is fixed as the total number of defect α at growth temperature. By solving all equations in Eqs. (2)–(5) self-consistently, we can get a new set of E_F, carrier densities, and defect densities with different charge states after the sample is quenched.

The right panels of Fig. 3 show the Fermi levels, carrier densities, and defect densities as functions of the Cd chemical potential after quenching in CdTe. The hole density for p-type CdTe after quenching is on the order of $10^{14}/\mathrm{cm}^3$, which agrees well with experiments. Notably, for p-type CdTe grown under Cd-poor conditions, the E_F^p is lowered after quenching while for n-type CdTe under Cd-rich conditions, the E_F^n is raised (see also Fig. 4). Our results are consistent with the previous work of Berding [34], in which Fermi level splitting in CdTe is also found to be enlarged after quenching, although in her local density approximation (LDA) calculation, the band gap is severely underestimated. Therefore, our calculations show that in the case of CdTe, after quenching from high growth temperatures, both E_F^n and E_F^p can been tuned beyond the self-doping limit under equilibrium growth conditions.

VI. DISCUSSIONS

The reason that E_F^p is pushed significantly past A after quenching under Cd-poor conditions can be understood as follows. At high growth temperatures with Cd-poor conditions, V_{Cd}^{2-} has a very low formation energy because the Fermi level is pinned at a position higher than A due to thermal excitation [Fig. 2(a)]. Therefore, it is dominant and has a much higher density than other defects. After quenching, the thermally excited electrons from the VBM to the conduction band maximum (CBM) of CdTe are dramatically reduced, but the existence of large amounts of V_{Cd} with negatively charged states close to the VBM makes holes dominant over electrons, thus pushing the Fermi level down towards the (0/2−) transition energy level of V_{Cd} at 0.36 eV and VBM. In this case, the defect level acts as a new "CBM" state when the defect density is high and the total density of V_{Cd} acts as "N_c." As is shown in Fig. 4(b), the quenched Fermi level initially decreases as the growth temperature increases, from 0.38 eV (600 K) to 0.35 eV (700 K) to 0.34 eV (800 K). This is due to the increased defect density of V_{Cd} as the growth temperature increases. However, further increases of growth temperature leads to an increase of the Fermi energy [Fig. 4(b)]. Because at very high growth temperatures, the densities of donor defects such as $\mathrm{Te}_{\mathrm{Cd}}^{2+}$ and V_{Te}^{2+} also increase significantly, leading to the slight increase in Fermi level after quenching. Besides, $\mathrm{Te}_{\mathrm{Cd}}$ has a deep (2+/0) transition energy level, and thus can serve as recombination centers, therefore, its density should be suppressed by either lowering growth temperature or growing CdTe under Cd-rich conditions. After taking all the above factors into consideration, we suggest that it's best to grow p-type doped CdTe at 800 K with $\mu_{\mathrm{Cd}} \sim -1.0$ eV, which gives an E_F^p of about 0.35 eV after quenching. Further tuning down of E_F^p can only be achieved by extrinsic impurities, which may create shallower transition energy levels than V_{Cd}.

The reason why E_F^n is tuned beyond B after quenching under Cd-rich conditions is analogous to the previous mechanism. At high growth temperatures with Cd-rich conditions, fully ionized V_{Te}^{2+} is the dominant defect because the Fermi energy is pinned close to the band gap center [Fig. 2(b)]. After quenching, the thermally excited electrons and holes from the VBM to the CBM of CdTe are dramatically reduced. The high density of V_{Te}^{2+} makes electrons dominant over holes and shifts the Fermi level towards the CBM. In this case, the hole density at the VBM disappears and the defect level of V_{Te} acts as a new "VBM" state and the total density of V_{Te} acts as "N_v." We note that the quenched E_F^n increases as the growth temperature increases. This is because the (2+/0) transition energy level of V_{Te} and $\mathrm{Cd}_{\mathrm{Te}}$ is above the CBM, so V_{Te} is always in the 2+ charged ionized state. The higher the growth temperature, the more V_{Te}^{2+} will be formed under equilibrium growth conditions. After quenching, V_{Te}^{2+} passivates the holes at the VBM and pushes the Fermi level upwards. Importantly, there are no low energy acceptor defects which can donate extras holes after Fermi energy increases, therefore, the quenched E_F^n is only limited by the CBM.

Our analysis suggests that quenching can selectively enhance the defect density of the desired dopants and suppress the undesired dopants, and therefore is an effective strategy to overcome Fermi level pinning caused by intrinsic defect self-compensation. By quenching, E_F^p has been significantly tuned downwards and E_F^n is pushed upward, thus ϕ_D, as well as the V_{OC}, is increased towards the band gap value. According to our calculations, if p-type CdTe is grown at 800 K at Cd-poor conditions, a Fermi level of 0.35 eV above the VBM can be obtained; likewise if n-type CdTe is grown at 1200 K under Cd-rich conditions, a quenching Fermi level of 1.42 eV can be

achieved. Therefore, a ϕ_D of 1.07 eV is, in principle, achievable by intrinsic doping alone, which could significantly improve the energy conversion efficiency of CdTe solar cells. In general, quenching from a higher growth temperature can lead to a higher ϕ_D [Fig. 4(b)] or larger Fermi level ranges. However, in practice, the growth temperature may be limited by factors such as melting point of the glass substrates thus limiting the achievable ϕ_D and V_{OC}.

VII. CONCLUSION

In conclusion, we have proposed an effective, nonequilibrium quenching method for overcoming the E_F limitation caused by self-compensation of intrinsic defects in semiconductor materials and make E_F cover a much wider range of the band gap. By applying this approach to CdTe, we show that the Fermi level range, thus the diffusion voltage ϕ_D, can increase significantly from about 0.6 to about 1.1 eV, which, therefore, has the potential to significantly improve its solar cell performance. The proposed strategy of tuning Fermi level positions beyond the intrinsic doping limit is based on simple thermodynamics, so it is general and can be applied to other semiconductor systems.

ACKNOWLEDGMENTS

The work at NREL is supported by the US Department of Energy, EERE/SunShot program, under Contract No. DE-AC36-08GO28308. The work at DGIST was supported by the DGIST MIREBraiN Program.

[1] Y. L. Chen, J. G. Analytis, J.-H. Chu, Z. K. Liu, S.-K. Mo, X. L. Qi, H. J. Zhang, D. H. Lu, X. Dai, Z. Fang, S. C. Zhang, I. R. Fisher, Z. Hussain, and Z.-X. Shen, Science **325**, 178 (2009).
[2] D. Hsieh, Y. Xia, D. Qian, L. Wray, J. H. Dil, F. Meier, J. Osterwalder, L. Patthey, J. G. Checkelsky, N. P. Ong, A. V. Fedorov, H. Lin, A. Bansil, D. Grauer, Y. S. Hor, R. J. Cava, and M. Z. Hasan, Nature (London) **460**, 1101 (2009).
[3] Y. Xia, D. Qian, D. Hsieh, L. Wray, A. Pal, H. Lin, A. Bansil, D. Grauer, Y. S. Hor, R. J. Cava, and M. Z. Hasan, Nat. Phys. **5**, 398 (2009).
[4] Y. Jiang, Y. Y. Sun, M. Chen, Y. Wang, Z. Li, C. Song, K. He, L. Wang, X. Chen, Q.-K. Xue, X. Ma, and S. B. Zhang, Phys. Rev. Lett. **108**, 066809 (2012).
[5] H. Fritzsche, Solid State Commun. **9**, 1813 (1971).
[6] D.-K. Ko and C. B. Murray, ACS Nano **5**, 4810 (2011).
[7] B. Paul, P. K. Rawat, and P. Banerji, Appl. Phys. Lett. **98**, 262101 (2011).
[8] C. S. Lue, Y.-K. Kuo, C. L. Huang, and W. J. Lai, Phys. Rev. B **69**, 125111 (2004).
[9] S.-H. Wei, Comput. Mater. Sci. **30**, 337 (2004).
[10] C. G. Van de Walle, D. B. Laks, G. F. Neumark, and S. T. Pantelides, Phys. Rev. B **47**, 9425 (1993).
[11] S.-H. Wei and S. B. Zhang, Phys. Rev. B **66**, 155211 (2002).
[12] S. B. Zhang, S.-H. Wei, and A. Zunger, J. Appl. Phys. **83**, 3192 (1998).
[13] S. B. Zhang and S.-H. Wei, Phys. Rev. Lett. **86**, 1789 (2001).
[14] X. Nie, S. B. Zhang, and S.-H. Wei, Phys. Rev. Lett. **88**, 066405 (2002).
[15] D. Segev and S.-H. Wei, Phys. Rev. Lett. **91**, 126406 (2003).
[16] A. Janotti, S.-H. Wei, and S. B. Zhang, Appl. Phys. Lett. **83**, 3522 (2003).
[17] S. Limpijumnong, S. B. Zhang, S.-H. Wei, and C.-H. Park, Phys. Rev. Lett. **92**, 155504 (2004).
[18] S. B. Zhang, S.-H. Wei, and A. Zunger, Phys. Rev. Lett. **84**, 1232 (2000).
[19] B. Huang, S. Chen, H.-X. Deng, L.-W. Wang, M. A. Contreras, R. Noufi, and S.-H. Wei, IEEE J. Photovoltaics **4**, 477 (2014).
[20] S. Chen, J.-H. Yang, X. G. Gong, A. Walsh, and S.-H. Wei, Phys. Rev. B **81**, 245204 (2010).
[21] M. A. Green, K. Emery, Y. Hishikawa, W. Warta, and E. D. Dunlop, Prog. Photovoltaics: Res. Appl. **20**, 12 (2012).
[22] http://investor.firstsolar.com/releasedetail.cfm?ReleaseID=828273
[23] P. Hohenberg and W. Kohn, Phys. Rev. **136**, B864 (1964).
[24] W. Kohn and L. J. Sham, Phys. Rev. **140**, A1133 (1965).
[25] G. Kresse and J. Furthmüller, Phys. Rev. B **54**, 11169 (1996).
[26] G. Kresse and J. Furthmüller, Comput. Mater. Sci. **6**, 15 (1996).
[27] G. Kresse and D. Joubert, Phys. Rev. B **59**, 1758 (1999).
[28] J. Heyd, G. E. Scuseria, and M. Ernzerhof, J. Chem. Phys. **125**, 224106 (2006).
[29] O. Madelung, M. Schulz, and H. Weiss (eds.), *Landolt-Bornstein: Numerical Data and Functional Relationships in Science and Technology*, Vol. 17b (Springer, Berlin, 1982).
[30] J. Ma, D. Kuciauskas, D. Albin, R. Bhattacharya, M. Reese, T. Barnes, J. V. Li, T. Gessert, and S.-H. Wei, Phys. Rev. Lett. **111**, 067402 (2013).
[31] S. Sze, *Physics of Semiconductor Devices*, 2nd ed. (Wiley, New York, 1981).
[32] J. Ma, S.-H. Wei, T. A. Gessert, and K. K. Chin, Phys. Rev. B **83**, 245207 (2011).
[33] R. Romestain and C. Weisbuch, Phys. Rev. Lett. **45**, 2067 (1980).
[34] M. A. Berding, Phys. Rev. B **60**, 8943 (1999).